reduced vibration amplitudes and a slight phase shift. However, the global-N_x model results show no phase shift and an increased vibration amplitude. Figure 4a shows the time history of the surface pressure for the two ε cases studied, 0.05 and 0.4, using the computed value of τ_w. Increasing ε results in increased surface pressure amplitudes and nonsymmetric fluctuations. Figure 4b shows the time histories of the wall shear stress. Similar to the pressure, the shear stress amplitudes increase with increasing ε and show the presence of additional frequencies. The increase in amplitudes is not as large as in the case of the pressure. Figure 5 shows the in-plane displacement response at the center of the beam for the same two cases and for the case with large wall shear stress and $\varepsilon = 0.4$. In all of the cases, the time histories show the presence of more than one frequency. As expected, the in-plane displacement response is orders of magnitude smaller than the out-of-plane one.

Conclusions

Results obtained in this study show that in flows producing large wall shear stresses, a fully coupled model that uses the local value of the tension, that is, a local-N_x model, and that accounts for wall shear stress is needed for accurate predictions of structural response. This result was shown to be true for both low- and high-pressure loading. In flows with low wall shear stresses, the global-N_x model is sufficient for accurate structural vibration predictions.

References

[1]Corcos, G. M., "Resolution of Pressure in Turbulence," *Journal of the Acoustical Society of America*, Vol. 35, No. 2, 1963, pp. 192–198.

[2]Chase, D. M., "Modeling the Wavenumber-Frequency Spectrum of Turbulent Boundary Layer Wall Pressure," *Journal of Sound and Vibration*, Vol. 70, No. 1, 1980, pp. 29–67.

[3]Leganelli, A. L., and Wolfe, H., "Prediction of Fluctuating Pressure in Attached and Separated Turbulent Boundary Layer Flow," AIAA Paper 89-1064, 1989.

[4]Efimtsov, B. M., "Characteristics of the Field of Turbulent Wall Pressure Fluctuations at Large Reynolds Numbers," *Soviet Physical Acoustics*, Vol. 28, No. 4, 1982, pp. 289–292.

[5]Graham, W. R., "A Comparison of Models for Wavenumber Frequency Spectrum of Turbulent Boundary Layer Pressures," *Proceedings of the First AIAA/CEAS Conference on Aeroacoustics* AIAA, Washington, DC, 1994, pp. 711–720.

[6]Vacaitis, R., Jan, C. M., and Shinozuka, M., "Nonlinear Panel Response from a Turbulent Boundary Layer," *AIAA Journal*, Vol. 10, No. 7, 1972, pp. 895–899.

[7]Wu, S. F., and Maestrello, L., "Responses of Finite Baffled Plate to Turbulent Flow Excitations," *AIAA Journal*, Vol. 33, No. 1, 1995, pp. 13–19.

[8]Frendi, A., and Robinson, J., "Effect of Acoustic Coupling on Random and Harmonic Plate Vibrations," *AIAA Journal*, Vol. 31, No. 11, 1993, pp. 1992–1997.

[9]Robinson, J., Rizzi, S., Clevenson, S., and Daniels, E., "Large Deflection Random Response of Flat and Blade Stiffened Carbon–Carbon Panels," AIAA Paper 92-2390, 1992.

[10]Maestrello, L., Frendi, A., and Brown, D. E., "Nonlinear Vibration and Radiation from a Panel with Transition to Chaos Induced by Acoustic Waves," *AIAA Journal*, Vol. 30, No. 11, 1992, pp. 2632–2638.

[11]Frendi, A., Maestrello, L., and Bayliss, A., "Coupling Between Plate Vibration and Acoustic Radiation," *Journal of Sound and Vibration*, Vol. 177, No. 2, 1994, pp. 207–226.

[12]Frendi, A., "Coupling Between a Supersonic Turbulent Boundary Layer and a Flexible Structure," *AIAA Journal*, Vol. 35, No. 1, 1997, pp. 58–66.

[13]Frendi, A., "Effect of Pressure Gradients on Plate Response and Radiation in a Supersonic Turbulent Boundary Layer," NASA CR-201691, 1997.

[14]Maestrello, L., "Radiation from and Panel Response to a Supersonic Turbulent Boundary Layer," *Journal of Sound and Vibration*, Vol. 10, No. 2, 1969, pp. 262–295.

[15]Frendi, A., Maestrello, L., and Ting, L., "An Efficient Model for Coupling Structural Vibrations with Acoustic Radiation," *Journal of Sound and Vibration*, Vol. 182, No. 5, 1995, pp. 741–757.

[16]Rumsey, C., Thomas, J., Warren, G., and Liu, G., "Upwind Navier–Stokes Solutions for Separated Periodic Flows," AIAA Paper 86-0247, 1986.

[17]Hoff, C., and Pahl, P. J., "Development of an Implicit Method with Numerical Dissipation from a Generalized Single-Step Algorithm for Structural Dynamics," *Computer Methods in Applied Mechanics and Engineering*, Vol. 67, No. 2, 1988, pp. 367–385.

E. Livne
Associate Editor

Absolute Instability of a Potential Flow over Plate–Spring System

Zhao Hanzhong*
Huazhong University of Science and Technology, 430074 Wuhan, People's Republic of China
and
K. S. Yeo†
National University of Singapore, 119260 Singapore, Republic of Singapore

Introduction

THE concept of using a compliant wall to reduce skin friction and flow noise has motivated a number of studies of instabilities that arise from the interaction between a passive compliant coating and a flow. In a series of experiments, Hansen et al.[1] and Gad-el-Hak et al.[2] observed the large-amplitude form of a static divergence (SD) wave on a highly damped viscoelastic layer under turbulent boundary layers. The onset of SD instability will lead to the temporal growth of the disturbance at any fixed point in the flow and is likely to give rise to significantly large surface vibrations or oscillations. This may cause a roughness effect that would directly increase the skin-friction drag and flow noise.

The SD instability mode is generally believed to be an absolute instability. The limited knowledge that we have of absolute instability over flexible plates has been derived primarily from a handful of works. For example, Brazier-Smith and Scott[3] found that potential flow over nondissipative compliant plates suffers from absolute instability when the flow speed exceeds a certain critical value, depending on the properties of the plate; Lucey and Carpenter[4] studied the response of a single-point pulse perturbation in an unsteady potential flow; and Yeo et al.[5,6] studied the absolute instability of laminar boundary layer and modified potential flows, representing turbulent and laminar boundary layers, over viscoelastic compliant layers.

The focus of the present Note is on uniform potential flow over a plate–spring system. Uniform potential flow represents the limiting form of laminar and turbulent boundary layers as their thickness tends to zero, and the plate–spring system may schematically describe a general theoretical model for a compliant wall. The numerical model is quite simple, but the study for this simple model allows us to better appreciate and understand the significance of the hydroelastic-type instabilities in a flow over compliant layer.

Mapping Technique to Detect Absolute Instability

The spatio–temporal evolution of a perturbation impulse located at the origin $x = 0$ is described by the following Green's function:

$$G(x, t) = \frac{1}{4\pi^2}\int_L\int_F \frac{\mathrm{d}\alpha\,\mathrm{d}\omega}{D(\alpha, \omega)}\exp(i\alpha x - i\omega t) \tag{1}$$

The complex frequency ω and complex wave number α are related by the dispersion relation $D(\alpha, \omega) = 0$. The time-asymptotic response of Green's function may be determined via a process of analytic continuation in which the Laplace contour L is deformed toward the real axis of the complex ω plane. When the Laplace contour L is deformed, the Fourier contour F is simultaneously deformed to preserve the analyticity of the integral if the paths of two α roots originating from opposite halves of the α plane intersect each other. We term such an intersection point a pinch point. The double α roots at the pinch point give rise to a singularity at the corresponding

Received 30 March 2000; revision received 28 September 2000; accepted for publication 23 October 2000.

*Associate Professor, Department of Mechanics; llyzys@public.wh.hb.cn.

†Associate Professor, Department of Mechanical and Production Engineering, Kent Ridge Crescent.

ω. The singularity in the ω plane is a branch point, with its branch cut taken straight down. When such a branch-point singularity occurs in the upper half of the ω plane, there is an absolute instability, that is, at all points in space,

$$\lim_{t\to\infty} G(x,t) \to \infty$$

Otherwise, there is at most convective instability so that

$$\lim_{t\to\infty} G(x,t) \to 0$$

A fuller account of the theory is given by Briggs[7] and Bers.[8]

Kupfer et al.[9] devised a useful procedure for locating the branch-point singularities of absolute instability. At a point of intersection of two α roots, the local mapping between the α plane and the ω plane has the form of quadratic equation. If α_0 is the intersection point in the α plane and ω_0 is the image of α_0 in the ω plane, the α_i contour that passes through α_0 forms a cusp at ω_0. When $(\omega_0)_i > 0$, a possible absolute instability is indicated. It is still necessary, however, to verify that the intersection arises from α roots originating from opposite halves of the α plane. This requirement can be checked by drawing a straight ray from the suspected cusp point ω_0 vertically upward ($\omega_r =$ cons) and observing the number of times this ray intersects the image of the α_r axis ($\alpha_i = 0$) in the ω plane. The sum total of crossings must be an odd number for a genuine branch-point singularity. This cusp-producing feature of the local map is an effective means for detecting the occurrence of α root interactions.

Dispersion Relation

A fairly general theoretical model for a compliant coating may be illustrated schematically by a plate–spring system. The plate–spring system consists of an elastic plate (or tensioned membrane) supported above a rigid surface by an array of springs, as shown in Fig. 1. A uniform potential flow is regarded to pass along the plate (or membrane) surface. If such a surface undergoes disturbances with the form of

$$\eta = \hat{\eta}\exp(i\alpha x - i\omega t) \tag{2}$$

the motion of the surface will be governed by the following nondimensional equation:

$$\gamma_w\left(\frac{\partial^2\eta}{\partial t^2} + d\frac{\partial\eta}{\partial t} + D\frac{\partial^4\eta}{\partial x^4} - T\frac{\partial^2\eta}{\partial x^2} + K_E\eta\right) = -p_s \tag{3}$$

where $\gamma_w = \rho_w/\rho$, where ρ_w is density of the plate and ρ is density of the fluid; d is nondimensional damping coefficient; D is nondimensional flexural rigidity; T is nondimensional longitudinal tension; and K_E is nondimensional spring stiffness. When flexural rigidity is taken as $D = 0$, it is a tensioned membrane case; when $T = 0$, it corresponds to an elastic plate. Here p_s are the perturbations in fluid pressure acting on the plate surface. It may be determined from a direct application of Bernoulli's theorem and the continuity of normal velocity at the interface as

$$p_s = -\alpha\ 1 - (\omega/\alpha)]^2\eta \tag{4}$$

in which the velocity of potential flow is taken as unity. Substituting p_s into Eqs. (3) obtains the solutions of this equation for radian frequency:

$$\omega = \frac{2 - id\gamma_w \pm \sqrt{(2 - id\gamma_w)^2 - 4(1+\alpha\gamma_w)\left[1 - \gamma_w\left(D\alpha^3 + T\alpha + K_E\alpha^{-1}\right)\right]}}{2(1+\alpha\gamma_w)}\alpha \tag{5}$$

It is the dispersion relation of a uniform potential flow over a plate–spring system. For given wave number α and prescribed plate and spring parameters, two branches of the ω solution can be obtained from this equation.

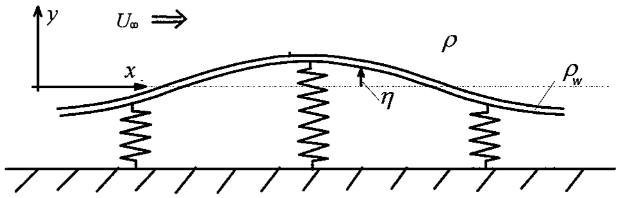

Fig. 1 Uniform potential flow over plate–spring system.

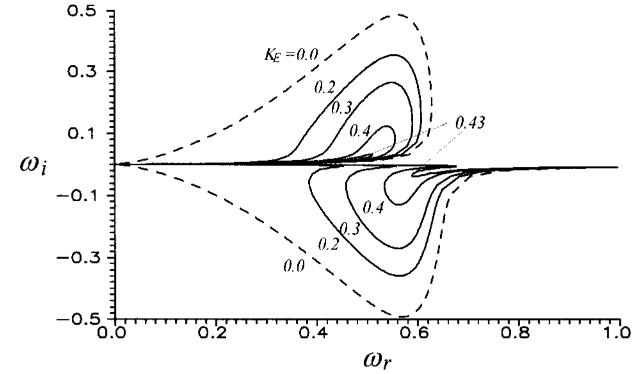

Fig. 2 Contours of $\alpha_i = 0$ at various spring stiffness for a bending plate; two branches of the contours locate at different halves of the ω plane.

Stability Analysis

We start the study from a damped bending plate ($T = 0$, $D \neq 0$) with $h = 1$, $\gamma_w = 1$, $d = 0.01$, and $D = 0.109$. The temporal stability is first investigated via solutions of the dispersion equation (5) for real wave number α. In a temporal theory, the instability occurs if there exists a root of the dispersion relation with $\omega_i > 0$ because positive ω_i indicates a temporal growth of the perturbation amplitude. Figure 2 shows $\alpha_i = 0$ contours for various spring stiffness K_E. The dispersion equation has two complex ω roots, one located in each half of the ω plane. Those located in the upper-half ω plane represent unstable temporal modes. The system is, thus, identified as being unstable. Figure 2 also shows that the $\alpha_i = 0$ contours form closed loops and cross the origin point $\omega = 0$. Increase in stiffness K_E causes the $\alpha_i = 0$ loop in the upper-half plane to tighten and shrink toward the origin $\omega = 0$. The $\alpha_i = 0$ loop eventually vanishes into the origin as K_E is increased to a threshold of 0.9891. The threshold of K_E is unaffected by the level of the damping.

The absolute instability is further examined via a spatio–temporal analysis. More α_i contours (for $\alpha_i \neq 0$) are mapped onto the ω plane through the dispersion relation (5). Figure 3 shows the mappings for the case of damped plate with spring stiffness $K_E = 0.2$ and damping coefficient $d = 0.01$. A cusp point is formed by the $\alpha_i = -0.105$ contour. The cusp point indicates the occurrence of root intersection in the corresponding α planes. The causality requirement may be verified by extending a straight line vertically upward from the cusp point and ascertaining the number of times the line intersects the $\alpha_i = 0$ contour. It is readily seen that such a straight line would intersect the said contour only once. This indicates that the unstable mode we found is also an absolutely unstable mode.

As spring stiffness K_E is increased, the $\alpha_i = 0$ loop shrinks toward the origin $\alpha_i = 0$. The shrinking of the loop takes place with the cusp point being entrapped within the loop throughout, as shown in Fig. 4. The loop eventually vanishes into the origin as K_E is increased to the threshold value, at which point the loop is itself transformed into the cusp that it encloses. There is, thus, no convectively unstable mode for a damped bending plate. Similar instability behavior was found

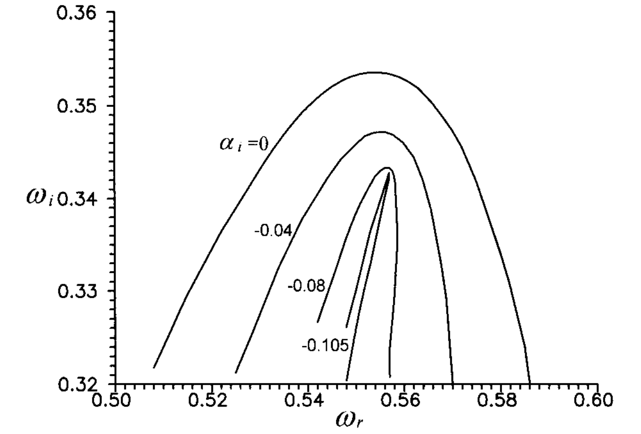

Fig. 3 Unstable branch of α_i contours for a damped bending plate; branch-cut singularity occurs.

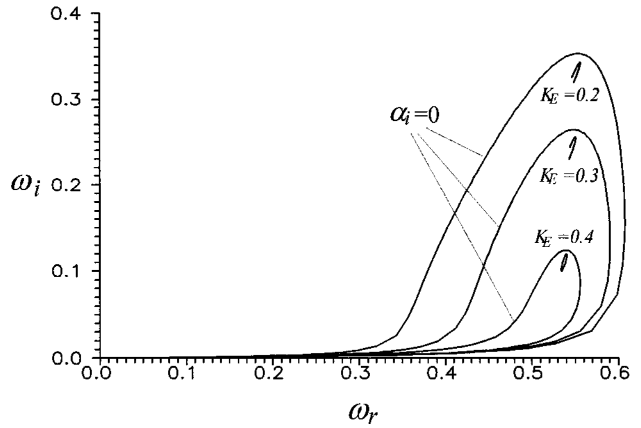

Fig. 4 Unstable branch of α_i contours for a damped bending plate; cusp point moves toward origin as spring stiffness is increased.

by Yeo et al.[6] in the potential flow over a single-layer viscoelastic wall.

On the other hand, no cusp points have been found at the α_i contours for an undamped plate ($d = 0$). All of the $\alpha_i \neq 0$ contours are discontinuous in upper-half plane; ω roots jump to the opposite side of the real axis before the contours form cusps. It, therefore, indicates that a potential flow over an infinitely long undamped bending plate does not admit absolute instability.

A similar situation can also be seen for a membrane ($T \neq 0$, $D = 0$). A potential flow over an undamped membrane admits static temporal instability, whereas a flow over damped membrane admits only an absolute instability mode.

Conclusions

The instability of a uniform potential flow over a plate–spring system is investigated from the time-asymptotic spatio-temporal perspective. The study indicates that uniform potential flow over damped plate–spring system admits only absolute instability modes. Absolute instability sets in as the flow becomes unstable according to normal-mode temporal theory, and the onset of instability for a damped plate (or membrane) is unaffected by the damping level. A potential flow over an undamped plate–spring system does not admit absolute instability.

References

[1]Hansen, R. J., Hunston, D. L., Ni, C. C., and Reischman, M. M., "An Experimental Study of Flow-Generated Waves on a Flexible Surface," *Journal of Sound Vibration*, Vol. 68, No. 2, 1980, pp. 317–334.

[2]Gad-el-Hak, M., Blackwelder, R. F., and Riley, J. J., "On the Interaction of Compliant Coatings with Boundary-Layer Flows," *Journal of Fluid Mechanics*, Vol. 140, 1984, pp. 257–280.

[3]Brazier-Smith, P. R., and Scott, J. F., "Stability of Fluid Flow in the Presence of a Compliant Surface," *Wave Motion*, Vol. 6, No. 3, 1984, pp. 547–562.

[4]Lucey, A. D., and Carpenter, P. W., "A Numerical Simulation of the Interaction of a Compliant Wall and Inviscid Flow," *Journal of Fluid Mechanics*, Vol. 234, 1992, pp. 121–156.

[5]Yeo, K. S., Khoo, B. C., and Zhao, H. Z., "The Absolute Instability of Boundary-Layer Flow Over Viscoelastic Walls," *Theoretical and Computational Fluid Dynamics*, Vol. 8, No. 2, 1996, pp. 237–252.

[6]Yeo, K. S., Khoo, B. C., and Zhao, H. Z., "The Convective and Absolute Instability of Fluid Flow Over Viscoelastic Compliant Layers," *Journal of Sound Vibration*, Vol. 223, No. 3, 1999, pp. 379–398.

[7]Briggs, R. J., *Electron-Stream Interaction with Plamas*, Monograph No. 29, MIT Press. Cambridge, MA, 1964, Chap. 2.

[8]Bers, A., *Handbook of Plasma Physics*, North-Holland, Amsterdam, 1983, Chap. 3.

[9]Kupfer, K., Bers, A., and Ram, A. K., "The Cusp Map in the Complex-Frequency Plane for Absolute Instabilities," *Physics of Fluids*, Vol. 30, No. 10, 1987, pp. 3075–3082.

P. J. Morris
Associate Editor

Effect of Addition of Radicals on Burning Velocity

Kenichi Takita* and Goro Masuya†
Tohoku University, Sendai 980-8579, Japan
Takahiro Sato‡
Hitachi–Zosen Company, Osaka 559-8559, Japan
and
Yiguang Ju§
Tsinghua University, Beijing 100084, People's Republic of China

Introduction

IT is well known that the addition of radicals to a combustible mixture drastically decreases the ignition delay time and extends the flame holding limit.[1] Therefore, many practical applications, for example, a plasma torch igniter for a scramjet engine[2] or ignition and flame holding by a laser, and enhancement of combustion by a continuous electric discharge,[3] have been developed to enhance ignition and flame stability. Although the effect of the addition of radicals on ignition delay time has been extensively investigated, little attention has been focused on its effect on burning velocity except for the case of flame propagation with oscillation in a closed chamber.[4] From the viewpoint of flame holding, a change in burning velocity by the addition of radicals may possibly play an important role. In this study, the effect of the addition of radicals on burning velocity was investigated using a one-dimensional flame code.

Numerical Method

Burning velocities with the addition of radicals were calculated using the one-dimensional flame code developed by Smooke et al.[5] A reaction model constituted from 15 (O_2, H_2, H_2O, H, HO_2, O, OH, H_2O_2, N_2, N, NO, NO_2, N_2O, NH, and HNO) species and 45 elementary reactions[6–8] was used in the calculations. The code and

---

Presented as Paper 99-2147 at the 35th Joint Propulsion Conference, Los Angeles, CA, 20–23 June 1999; received 20 April 2000; revision received 20 November 2000; accepted for publication 1 December 2000.

*Assistant Professor, Department of Aeronautics and Space Engineering; takita@cc.mech.tohoku.ac.jp. Member AIAA.

†Professor, Department of Aeronautics and Space Engineering. Senior Member AIAA.

‡Researcher, Department of Environmental System and Technology.

§Professor, Department of Engineering Mechanics.